Electromagnetic Interactions of Metallic Objects in Nanometer Proximity

R. Berndt* and J. K. Gimzewski
IBM Research Division, Zurich Research Laboratory, CH-8803 Rüschlikon, Switzerland

P. Johansson
NORDITA, Blegdamsvej 17, DK-2100 Copenhagen Ø, Denmark
(Received 10 August 1993)

The chemical and proximity dependence of electromagnetic interactions of various metallic bodies at nanometer separations is probed through photon emission from a scanning tunneling microscope. The role of local dielectric properties is determined and the strength of the electromagnetic coupling in the cavity between tip and sample is investigated. The experimental results compare well with model calculations and show the relative role of the dielectric functions of both electrodes as well as the influence of proximity.

PACS numbers: 61.16.Ch, 73.40.Gk, 78.60.Fi

Recent experiments with scanned probe microscopies have demonstrated the fabrication of structures on surfaces with dimensions in the nanometer range [1]. These structures are hoped to exhibit interesting physical properties compared with those of bulk materials owing to modifications of their elementary excitations. The scanning tunneling microscope (STM) introduces the ability to perform local experiments to explore such phenomena.

We demonstrated in a recent Letter that the close proximity of tip and sample in the STM gives rise to dipolar tip-induced plasmons (TIP). These are localized electromagnetic modes which can be readily excited by inelastic electron tunneling [2,3]. Optical emission from TIP modes provides a direct probe of the electromagnetic interaction of two mesoscopic objects in nanometer proximity for which a theoretical model can be established. The phenomena of surface-enhanced Raman scattering (SERS) [4] are examples of a system that is critically influenced by similar local electromagnetic interactions. Such interactions also play an important role for clusters [5] and nanostructured materials [6]. The resonance frequency and the strength of TIP modes are determined by a variety of factors, which are experimentally accessible using photon emission from tunneling junctions. The geometry of the tip-sample region on a length scale given by the lateral extent of TIP modes and by the tip-sample distance is relevant for the electromagnetic coupling, and the system can be considered a model cavity structure. The TIP mode is determined by the dielectric properties of tip and sample material as well as the radius of the tip R and the gap spacing s.

To test these concepts directly, we used optical spectroscopic techniques to investigate the effect of the tip material on photon emission. We performed simultaneous measurements of tunneling characteristics and photon emission spectroscopy to study the distance dependence of the electromagnetic enhancement within the cavity of tip and sample. The experimental results are compared with model calculations.

The experimental configuration we use has been described in detail previously [7]. Briefly, our custom-built STM is surrounded by an ellipsoidal mirror to focus light from the tip region, which lies in the principal focus of the reflector, in the second focal point outside the vacuum chamber. Photomultipliers or a grating spectrometer and intensified diode array detector are used to detect and spectrally resolve the emission. Tip and sample preparation and experimentation were performed under ultrahigh vacuum (UHV) conditions (base pressure in the 10^{-11} mbar range). It should be noted that under ambient conditions the accessible range of tunneling voltages and currents is severely limited by instabilities due to junction breakdown involving material transfer between tip and sample [8]. Ag(111) and Au(110) surfaces were prepared by repeated cycles of Ne ion bombardment and subsequent annealing. X-ray photoelectron spectroscopy and low-energy electron diffraction were used to monitor surface contamination and ordering. Etched W tips were heated in UHV to 1000 K and then sharpened by Ne ion bombardment. Noble metal tips were prepared by evaporating thick layers ($d \approx 1000$ Å) of Ag or Au onto W tips.

The important role in photon emission played by the tip manifests itself in modifications of emission spectra depending on the tip material. Figure 1 displays the effect of tip materials on optical emission spectra from Ag(111) surfaces. Spectrum (a) was measured with a W tip and exhibits a single, broad maximum with a tail extending far into the long wavelength range. Although the tip plays a crucial role by inducing a coupled mode, the dielectric properties of the W tip do not give rise to pronounced structures in fluorescence spectra. This we ascribe to the nature of the dielectric function ϵ of W in the visible range, which exhibits strong damping as is evident from the large imaginary part of ϵ. Consequently, the tip material in this case mainly affects the width of the emission peak. For a Ag-covered tip [Fig. 1(b)], however, strikingly different emission characteristics are found using identical tunneling parameters. Two intensity maxima at 550 and 670 nm are clearly visible. The

0031-9007/93/71(21)/3493(4)$06.00

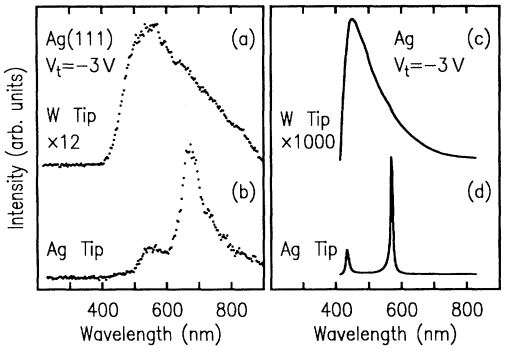

FIG. 1. Effect of tip material on fluorescence spectra from Ag(111) surfaces. (a) and (b) display experimental results at a tip voltage of $V_t = -3$ V for W and Ag tips. (c) and (d) show the corresponding theoretical findings. Spectra have been normalized using the factors given in the figure.

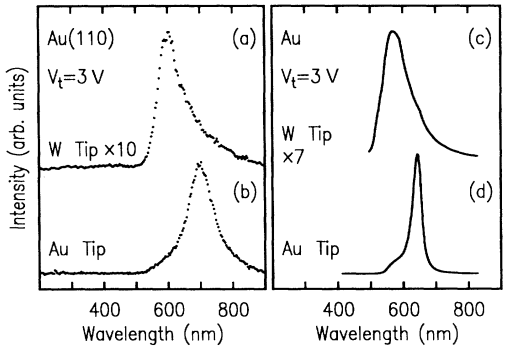

FIG. 2. Effect of tip material on fluorescence spectra from Au(110) surfaces. (a) and (b) display experimental results for W and Au tips. (c) and (d) show the theoretical findings for identical bias. Spectra have been normalized using the factors given in the figure.

peaks in Fig. 1(b) are significantly sharper (full width at half maximum < 70 nm) than the maximum in 1(a), and the intensity is higher by more than 1 order of magnitude. The peak positions as well as intensities varied strongly when measured with different Ag-covered tips but the intensities were consistently higher than those measured with W tips. The spectra measured with various W tips, in contrast, show consistent similarities to each other in both spectral structure and intensity. For a single Ag tip, variations in spectra are observed occasionally and can be attributed to structural instabilities of these tips when tunneling.

Figures 1(c) and 1(d) show theoretical model calculations of photon spectra for W and Ag tips (tip radius $R = 300$ Å) on a Ag surface for the same bias voltage where the detector response has been included in the calculation [9]. The qualitative similarity between experiment and theory is encouraging considering that we have not attempted to optimize the fit. First, due to the instabilities of Ag tips mentioned above, the dimensions of a particular tip are not known experimentally. Second, our nonretarded calculations are valid for tip radii $R \lesssim 500$ Å. For a Ag tip, the model predicts several well-resolved emission peaks as observed experimentally. The lowest-energy resonance occurs when approximately half of a wavelength of an interface plasmon between two flat Ag surfaces fits into the cavity formed between tip and sample surface. The radius of this cavity is approximately equal to the distance away from the symmetry axis where the tip-sample separation is twice its minimal value. The additional peaks at higher photon energies result from higher-order modes having nodes inside the cavity. For a Ag tip both the theoretical and experimental emission spectra are redshifted with respect to those obtained with a W tip. This may be understood qualitatively as follows: The W tip has no well-defined plasmon modes of its own and its role in the formation of the interface plasmon is passive. Ag tips, on the other hand, have unique plasmon resonances which on approaching a Ag surface couple with sample plasmon modes. Hence, coupled TIP modes acquire lower frequencies.

The measured emission lines for Ag tips are sharper and more intense than the ones observed with W tips. This is mainly due to the smaller internal damping in Ag. The difference between Ag tips and W tips is even more pronounced in the theoretical results. Likely reasons for this difference between theory and experiment are (i) in the experiment the inner part of the tip is W, which is strongly damping; (ii) the Ag coating leads to additional damping due to surface scattering; and (iii) the Ag-Ag cavity is a high-quality oscillator. Consequently radiation damping, which is not included in our nonretarded theory, becomes important.

We performed similar experiments on a Au surface [Figs. 2(a) and 2(b)] with a W tip and a Au-covered tip. As for Ag, the emission intensity increases by 1 order of magnitude when the tip is covered with Au and the Au-Au emission maximum is shifted to a wavelength which is $\approx$100 nm longer than for W-Au in agreement with the qualitative argument given above for Ag on Ag. We also note that the sharp drop in intensity observed at $\lambda \approx 550$ nm with a W tip is replaced by a shoulder for the Au-Au junction. The observed redshift, the change in spectral shape, and the variation in emission intensity are closely reproduced in the theoretical data calculated for identical tunneling parameters [Figs. 2(c) and 2(d)] lending further support to our interpretation.

Measurements of total photon intensity as a function of tunneling voltage, conducted in air, have been reported for several combinations of tip and sample materials [10]. These results differ from results obtained in UHV with isochromat spectroscopy, which was performed over a wide range of photon energies [11,12]. We attribute these differences of measurements in air most notably to the effects of contamination and the resulting tunneling characteristics as well as to electrical breakdown at elevated

voltages.

The observability of photon emission from metal surfaces in the STM operated in the tunneling regime is a direct consequence of the high electromagnetic field strength of TIP modes confined in the narrow cavity between tip and sample. The field enhancement of TIP modes may be readily explored by varying the tip-sample distance in a controlled manner. Variation of the tunneling gap also gives rise to a variation in tunneling current. Simultaneous measurements of the tunneling current and the isochromat photon intensity as a function of tip-sample distance consequently provide a unique probe into the role of the geometry of the cavity and is displayed in Fig. 3(a) for a W tip on Cu(111). To obtain these data the STM feedback loop was temporarily disabled and the vertical tip position was varied while current and intensity were recorded at constant tip voltage V_t. The tunneling current [lower curve in Fig. 3(a)] displays an exponential dependence on distance. The detected isochromat intensity [upper curve in Fig. 3(a)] also exhibits a very similar dependence on distance as expected. The measured photon intensity is, however, not exactly proportional to the tunneling current.

To emphasize this deviation the photon yield is shown in Fig. 3(b). Despite the scatter of the data a decrease in yield with increasing distance is visible over the range of tip excursion used (2 Å). In our model, the intensity reduction per angstrom calculated from the experimental parameters used [cf. solid line in Fig. 3(b)] is ≈7%, which is in close agreement with the experimental observation. The decrease of the field enhancement in the cavity between tip and sample is predicted to result in a larger drop of the emitted intensity (≈ 30%/Å). However, with a larger gap between tip and sample, tunneling electrons interact with the TIP mode over longer distances [13]. Consequently, the effect of the reduced field enhancement on the photon yield is compensated to some extent by the longer tunneling distance between tip and sample which enters the calculation through the transition matrix elements between initial and final states.

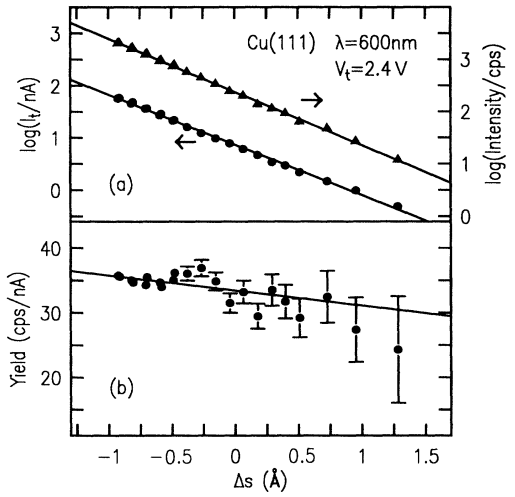

FIG. 3. (a) Simultaneous measurement of current I_t (circles) and isochromat photon intensity (λ = 600 nm) (triangles) as a function of vertical tip displacement Δs at fixed tip bias V_t = 2.4 V. A W tip was used on a Cu(111) surface. The initial tip-sample distance (Δs = 0) is determined by the tunneling parameters set before disabling the STM feedback loop (V_t = 2.4 V, I_t = 8 nA). $\Delta s > 0$ corresponds to increased tip-sample distance. Straight lines have been fitted to both data sets. (b) Yield (defined as intensity divided by current). The result of our model calculation (scaled by an arbitrary factor in the y direction and shifted in the x direction) is represented by a solid line.

The data in Fig. 3 permit a direct comparison of tunneling characteristics of the elastic and inelastic channels. From the variation of the tunneling current I_t with tip displacement Δs, an apparent barrier height Φ_{et} may be deduced according to $\Phi_{et}(\mathrm{eV}) = 0.952[d \ln I(\mathrm{A})/ds(\mathrm{Å})]^2$ [14]. Φ_{et} may be considered a property of the elastic tunneling channels since the tunneling current is predominated by their contributions [2]. Photons, however, are generated by electrons which tunnel inelastically [2,3], suggesting that an apparent barrier height for inelastic tunneling Φ_{iet} can be derived from the intensity data. It is important to note that a change in tip-sample distance affects the strength of tip-induced modes as demonstrated above; the photon emission spectrum for Cu, however, remains nearly unaffected. The behavior of I_t at small tip-sample separations [cf. Fig. 3(a)] indicates that no collapse of the apparent barrier Φ_{et} occurs in the range covered by our experiment. This permits us to equalize the tip excursion which is controlled experimentally with the actual change in tip-sample distance. From Fig. 3(a) we obtain Φ_{et} = 3.8 eV. Similarly, from the photon intensity curve [Fig. 3(b)], we calculate an apparent barrier height for the inelastic photon signal Φ_{iet} = 3.8 eV. The deduced barrier heights for the elastic and inelastic channels are identical within the experimental uncertainty.

At first glance, identical barrier heights for elastic and inelastic channels contradict the simple expectation that an electron suffering an energy loss should "see" a higher tunnel barrier given that the matrix elements for inelastic tunneling involve final states with an energy that is ~2–2.5 eV below the initial state [15]. On the basis of our experimental and theoretical evidence we propose a mechanism that explains why observed elastic and inelastic barrier heights are similar. An electron tunneling inelastically transverses most of the tunnel barrier at its initial energy and then it emits a photon. In effect it encounters a similar barrier as an electron tunneling elastically. In the quantum mechanical calculation this causes the transition matrix elements for inelastic processes to obtain their largest contribution from the region of the tunneling gap closest to the electron-collecting electrode.

A related observation is known from inelastic tunneling spectroscopy of molecular vibrational modes, where a clear asymmetry in peak height in d^2I_t/dV_t^2 spectra was observed depending on bias polarity [16].

In summary, the electromagnetic interaction of two metallic bodies in nanometer proximity has been investigated by observing photon emission from an STM. The chemical role of junction materials has been illustrated by measuring of fluorescence spectra using different tip-sample combinations. Comparison of the experimental results with model calculations yields a qualitative agreement of both spectral shape and relative intensities for Au and W tips with Au substrates, and qualitative similarities for Ag and W tips on Ag. These findings provide evidence that tip-induced plasmon modes are sensitive probes for the electromagnetic properties of nanoscopic cavities. Tunneling characteristics and isochromat spectroscopy are used to illustrate that these modes, which are similar to those active in the classical description of SERS, can be readily adjusted by changing experimental parameters such as the cavity geometry and chemical composition.

We thank Alexis Baratoff for many discussions. Expert experimental assistance by Reto R. Schlittler is gratefully acknowledged.

* Present address: Institut de Physique Expérimentale, Université de Lausanne, CH-1015 Lausanne, Switzerland.

[1] J.A. Stroscio and D.M. Eigler, Science **254**, 1319 (1991); C.F. Quate, in *Highlights in Condensed Matter Physics and Future Prospects*, edited by L. Esaki, NATO ASI Ser. B, Vol. 285 (Plenum Press, New York, 1991), p. 573.

[2] R. Berndt, J.K. Gimzewski, and P. Johansson, Phys. Rev. Lett. **67**, 3796 (1991).

[3] B.N.J. Persson and A. Baratoff, Phys. Rev. Lett. **68**, 3224 (1992).

[4] A. Otto, I. Mrozek, H. Grabhorn, and W. Akemann, J. Phys. Condens. Matter **4**, 1143 (1992).

[5] Proceedings of the 6th International Symposium on Small Particles and Inorganic Clusters, "ISSPIC-6," Chicago, Illinois, 16–22 September 1992 [Z. Phys. D (to be published)].

[6] Proceedings of the 1st International Conference on Nanostructured Materials, Cancun, Mexico, 22–26 September 1992 [J. Nanostruct. Mater. (to be published)].

[7] R. Berndt, R.R. Schlittler, and J.K. Gimzewski, J. Vac. Sci. Technol. B **9**, 573 (1991).

[8] V. Sivel, R. Coratger, F. Ajustron, and J. Beauvillain, Phys. Rev. B **45**, 8634 (1992).

[9] The model calculation is described in P. Johansson, R. Monreal, and P. Apell, Phys. Rev. B **42**, 9210 (1990); P. Johansson and R. Monreal, Z. Phys. B **84**, 269 (1991).

[10] I.I. Smolyaninov, V.S. Edelman, and V.V. Zavylow, Phys. Lett. A **158**, 337 (1991).

[11] J.H. Coombs, J.K. Gimzewski, B. Reihl, J.K. Sass, and R.R. Schlittler, J. Microscopy **152**, 325 (1988).

[12] R. Berndt and J.K. Gimzewski, Ann. Phys. (Leipzig) **2**, 133–140 (1993).

[13] As a consequence of the dielectric properties of tip and sample materials the electric field of a TIP mode is considerably stronger in the vacuum gap than in the metals.

[14] N.D. Lang, Phys. Rev. B **37**, 10 395 (1988).

[15] R. Berndt, A. Baratoff, and J.K. Gimzewski, in *Scanning Tunneling Microscopy and Related Methods*, edited by R.J. Behm, N. Garcia, and H. Rohrer, NATO Advanced Studies Institutes Ser. E, Vol. 184 (Kluwer, Dordrecht, 1990), p. 269.

[16] E.L. Wolf, *Principles of Electron Tunneling Spectroscopy* (Oxford University Press, New York, 1985), p. 443.